AMME3500 Design Project 2
Learjet 25 Pitch Control

Tom Bullock
SID: 530754154

I. Introduction

The pitch of an aircraft is a critical flight parameter that is responsible for many flight operations such as climb, descent and cruise. It is key that an aircraft maintains the desired pitch during all stages of flight to be able to carry out a successful flight mission. During safety critical parts of the flight, such as take-off and landing, the pilot must be at the yoke and largely responsible for the control of the aircraft. During cruise, however, demanding the pilot's full focus is unrealistic, especially for long haul flights. The reason is twofold: it is generally not possible for someone to maintain maximum concentration for extended periods of time, and more importantly, the less fatigued the pilot is when the aircraft is required to land, the better. As safety is paramount in aviation, due to the fact that if something goes wrong potentially catastrophic events can proceed, anything that increases the safety of the aircraft during flight is sought after. This outlines the motivations for the development of an aircraft autopilot pitch controller. The pitch controller will be utilised during the cruise phase of flight. This will relieve the pilot of these duties, reducing their workload, allowing the pilot to be more fresh either for landing or for whatever situation may arise; increasing the safety of flight.

The report begins by outlining the equations of motion of an aircraft, namely the six degrees of freedom (6DOF) equations. Proceeding to this, explanations on how the six highly non-linear coupled equations were simplified down to a more palatable form, from which a linearised state space model was developed. The system model was made 'real' by developing it around a Learjet25, which is representative of a subsonic business jet. An integral state was implemented into the state space model in anticipation of constant unknown disturbances such as headwinds. The integral state allows the aircraft to track a reference pitch perfectly despite unknown flight conditions, a desirable property. The controller was then designed, finding appropriate gains for the K matrix, and the system was stability confirmed. Following this, the system was analysed in SIMULINK and the controller was tested in various ways, which confirmed its robustness and ability to meet the design specifications. Finally, a conclusion of results and findings are presented.

The controller achieved its objectives in controlling the pitch of the aircraft in a realistic way with no steady state error. The usefulness of these results, however, are questionable simply due to the model simplifications that were used.

II. System Model and Problem Definition

A. Aircraft Equations of Motion

An aircraft's equations of motion are obtained by applying Newton's 2nd law of motion to a rigid body aircraft relative to a fixed inertial frame of reference. An inertial reference frame is an axis system that is fixed in space, for this purpose the Earth's axis system was used. This is not strictly an inertial reference frame due to the rotation of the Earth, however this is negligible in comparison to the rotation rates of the aircraft. When developing the equations of motion for an aircraft, four coordinate systems are often used: the Earth fixed axes system, the body-fixed axes system, the local horizon axes system and the wind axes system. The body-fixed axes is shown in Figure 1 along with the various force, moment and velocity components that act on an aircraft.

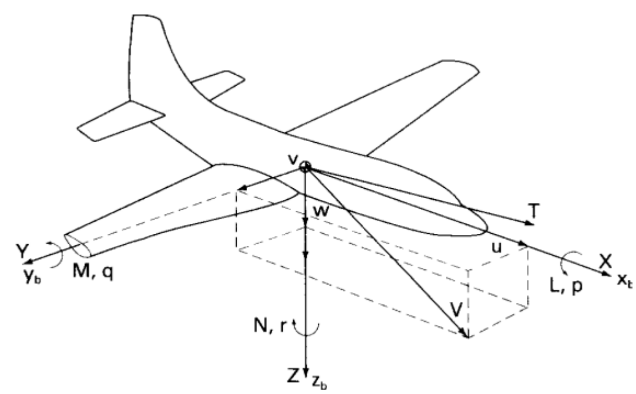

Fig. 1: Free body diagram of an aircraft in the body-fixed axis. Reproduced from [1].

TABLE I: Aircraft Nomenclature

	Roll Axis [x_b]	Pitch Axis [y_b]	Yaw Axis [z_b]
Angular Rates	p	q	r
Velocity	u	v	w
Net Force	X	Y	Z
Net Moment	L	M	N
Moment of Inertia	I_{xx}	I_{yy}	I_{zz}
Product of Inertia	I_{yz}	I_{xz}	I_{xy}

As shown in Figure 1, there are six possible degrees of freedom for an aircraft, a rotation and translation for each axis in three-dimensional space. The derivation of which is out of scope of this report, but they are provided to show the simplification process [1]:

The force equations:

$$X - mg\sin(\theta) = m(\dot{u} + qw - rv)$$
$$Y + mg\cos(\phi)\sin(\theta) = m(\dot{v} + ru - pw)$$
$$Z + mg\cos(\theta)\cos(\phi) = m(\dot{w} + pv - qu)$$

The moment equations:

$$L = I_x\dot{p} - I_{xz}(\dot{r} + qr(I_z - I_y)) - I_{xz}pq$$
$$M = I_y\dot{q} + r(I_x - I_z) + I_{xz}(p^2 - r^2)$$
$$N = -I_{xz}\dot{p} + I_z\dot{r} + pq(I_y - I_x) + I_{xz}qr$$

The system of equations presented that describe aircraft dynamics are highly nonlinear and coupled, therefore will have to be simplified to allow linear control methods to be implemented.

The coupled nature of the system was removed by assuming that the aircraft was not rotating, therefore the angular rates become 0. The control surfaces were assumed to not affect the lift and drag.

The pitching motion of the aircraft was assumed to be governed by the longitudinal dynamics, while the roll and yaw motion are governed by the lateral dynamics. This is generally an accurate assumption to make due to the coupling of the roll and yaw control surfaces. For example, when the rudder is used to control the yaw of the aircraft, it induces a relative velocity between the two wings which results in a relative lift and hence a roll motion. A similar coupling is seen with the ailerons, the roll control surfaces, as they contribute differential amounts of drag depending on which direction they are deflected which results in a relative forward velocity between the wings and hence a yawing motion.

The following non-linear longitudinal equations of motions were developed from the assumptions discussed [2]:

$$X_A + X_T = m\dot{u} + mgsin\theta$$
$$M_A + M_T = \dot{q}I_{yy}$$
$$Z_A + Z_T = m\dot{w} - mgcos\theta cos\phi$$

The aerodynamic and thrust contributions to forces and moment have been separately defined to aid the following section.

The linearization process is not trivial and as it's not the focus of this report it has been omitted, however the steps will be outlined. The 'small peturbation' approach was used where each variable was recast in terms of a steady state value and a perturbed value and expanded out. The products of small perturbations were assumed to be negligible and small angle approximations were used. The thrust was assumed to be constant. Following this, a first order Taylor series was used to approximate how the longitudinal perturbed aerodynamic forces and moments vary as a function of the five perturbed variables, due to the fact:

$$\Delta X_A, \Delta M_A, \Delta Z_A = f\left(\delta u, \delta\alpha, \delta\dot{\alpha}, \delta q, \hat{\delta_e}\right)$$

Where α is the angle of attack and δ_e is the elevator deflection, $\hat{\delta_e}$ is the perturbed elevator deflection.

The steady state (trim) condition for flight was chosen to be at steady cruise at constant altitude. It was also assumed that a change in pitch angle would not change the velocity of the aircraft. This was the most unrealistic of all the assumptions, it was made to keep the problem single-input-single-output (SISO). The alternative would result in a throttle input to keep the aircraft at the constant altitude flight condition.

This resulted in the following simplified longitudinal dynamical equations of motion [3]:

$$\dot{\alpha} = \mu\Omega\sigma\Bigg[-(C_L + C_D)\alpha + \frac{1}{(\mu - C_L)}q - \big[(C_W\sin\gamma)\theta + C_L\big]\delta_e\Bigg] \quad (1)$$

$$\dot{q} = \frac{\mu\Omega}{2i_{yy}}\Bigg[\left(C_M - \eta(C_L + C_D)\right)\alpha + \left(C_M + \sigma C_M(1 - \mu C_L)\right)q + (\eta C_W\sin\gamma)\delta_e\Bigg] \quad (2)$$

$$\dot{\theta} = \Omega q \quad (3)$$

Where C_L, C_D, C_M and C_D are the coefficients of lift, drag, moment and weight, respectively. The γ term is the flight path angle, which is a constant $0°$, given the straight and level flight condition. The α term is the angle of attack, i_{yy} is the normalized moment of inertia in the longitudinal axis and θ and q are the pitch and pitch rate, respectively.

Additionally, the following constants have been defined:

$$\eta = \mu\sigma C_M$$
$$\mu = \frac{\rho S\bar{c}}{4m}$$
$$\Omega = \frac{2U}{\bar{c}}$$
$$\sigma = \frac{1}{1 + \mu C_L}$$

B. System Model

The Learjet 25, which is representative of a standard subsonic business jet (SBJ), has the following properties at steady level flight at cruising altitude of 30 000 ft [4].

TABLE II: Learjet 25 Cruising Parameters

Parameter	Value
C_M [-]	0.6
C_L [-]	0.299
C_D [-]	0.0295
Wing Area (S) [m^2]	21.6
Mass (m) [kg]	4991
Cruise Velocity (U) [ms^{-1}]	182
Air Density (ρ) [kgm^{-3}]	0.4582
Mean Aerodynamic Chord ($\bar{c}$) [m]	2.13
i_{yy} [-]	0.1048

Substituting the aircraft parameters into the linearized longitudinal dynamic equations results in the following:

$$\dot{\alpha} = -0.05926\alpha - 0.60547q - 0.053938\delta_e \tag{4}$$

$$\dot{q} = 1.4228 \times 10^{-4}\alpha + 2.8578 \times 10^{-4}q \tag{5}$$

$$\dot{\theta} = 170.89\ q \tag{6}$$

1) State Space

The system model can be formed in a state space model in preparation for controller development:

$$\dot{x} = Ax + Bu \tag{7}$$

$$y = Cx + Du \tag{8}$$

Where the system is SISO if both u and y are scalars, the elevator angle will be the control input and the pitch angle is the output:

$$\begin{bmatrix} \dot{\alpha} \\ \dot{q} \\ \dot{\theta} \end{bmatrix} = \begin{bmatrix} -0.0593 & -0.6055 & 0 \\ 0.00014 & 0.0003 & 0 \\ 0 & 170.89 & 0 \end{bmatrix} \begin{bmatrix} \alpha \\ q \\ \theta \end{bmatrix} + \begin{bmatrix} -0.053 \\ 0 \\ 0 \end{bmatrix} \delta_e \tag{9}$$

$$y = \begin{bmatrix} 0 & 0 & 1 \end{bmatrix} \begin{bmatrix} \alpha \\ q \\ \theta \end{bmatrix} \tag{10}$$

C. Problem Definition

The pitch of an aircraft is the angle between the body-fixed x-axis and the earth-fixed x-axis. The pitch angle is a crucial parameter for many reasons such as in altitude control, for example climbing and descending are both controlled through adjusting the pitch of the aircraft. Additionally, maximum fuel efficiency requires the aircraft to be flying optimally, of which the pitch plays a large role. Passenger comfort is largely dictated by how 'smooth' the flight is, therefore sudden jolts in pitch would not be desirable. The pilot is capable of adjusting the elevator themselves through constant pull or push of the yoke, which is fine for short periods of time such as take-off and landing. However, this form of elevator control is not suitable for long periods of time as it causes pilot fatigue, which reduces the general safety of the flight. These reasons further outline the motivation for the development of a pitch control autopilot system.

III. Solutions and Numerical Validations

A. Integral State

The system model, developed in Section II-B, is now of an appropriate form for the development of a state feedback controller. However, given the nature of the pitch control application it is likely that the controller will be required to operate in conditions where there is a constant headwind of unknown strength for example, this can be modelled as a constant unknown disturbance. It is desirable that the pitch controller will be able to track a reference pitch without steady state error regardless of aircraft operating conditions, therefore an integrator state will be developed prior to controller design as this will allow the controller to meet the design requirements.

The integral state, z, is the integral of the error through time and takes the form:

$$z = \int_0^t y(\tau) - \theta_{ref}(\tau)\ d\tau \tag{11}$$

Differentiating Equation 11 removes the integral and transforms it into a form that can be put into the state space model, which gives the following:

$$\dot{z} = y - \theta_{ref} \tag{12}$$

Recalling that $y = Cx$ from Equation 8, Equation 12 becomes:

$$\dot{z} = Cx - \theta_{ref} \tag{13}$$

Adding this state to the model developed in II-B gives Equation 14:

$$\begin{bmatrix} \dot{x} \\ \dot{z} \end{bmatrix} = \begin{bmatrix} A & 0 \\ C & 0 \end{bmatrix} \begin{bmatrix} x \\ z \end{bmatrix} + \begin{bmatrix} B \\ 0 \end{bmatrix} u + \begin{bmatrix} 0 \\ -1 \end{bmatrix} \theta_{ref} \tag{14}$$

Where θ_{ref} is the desired pitch, the total state space model now becomes:

$$\begin{bmatrix} \dot{\alpha} \\ \dot{q} \\ \dot{\theta} \\ \dot{z} \end{bmatrix} = \begin{bmatrix} -0.0593 & -0.6055 & 0 & 0 \\ 0.00014 & 0.0003 & 0 & 0 \\ 0 & 170.89 & 0 & 0 \\ 0 & 0 & 1 & 0 \end{bmatrix} \begin{bmatrix} \alpha \\ q \\ \theta \\ z \end{bmatrix} + \begin{bmatrix} 0.053 \\ 0 \\ 0 \\ 0 \end{bmatrix} \delta_e + \begin{bmatrix} 0 \\ 0 \\ 0 \\ -1 \end{bmatrix} \theta_{ref} \tag{15}$$

The output becomes:

$$y = \begin{bmatrix} 0 & 0 & 1 & 0 \end{bmatrix} \begin{bmatrix} \alpha \\ q \\ \theta \\ z \end{bmatrix} \tag{16}$$

B. Controller Design

A state feedback controller was designed of the form:

$$u = -Kx = \begin{bmatrix} -K & -K_I \end{bmatrix} \begin{bmatrix} x \\ z \end{bmatrix} \tag{17}$$

Substituting this controller into Equation 14, the closed loop dynamics become:

$$\begin{bmatrix} \dot{x} \\ \dot{z} \end{bmatrix} = \begin{bmatrix} A - BK & -BK_I \\ C & 0 \end{bmatrix} \begin{bmatrix} x \\ z \end{bmatrix} + \begin{bmatrix} 0 \\ -1 \end{bmatrix} \theta_{ref} \tag{18}$$

If the system is stable, the steady state values become:

$$\begin{bmatrix} 0 \\ 0 \end{bmatrix} = \begin{bmatrix} A - BK & -BK_I \\ C & 0 \end{bmatrix} \begin{bmatrix} x_{ss} \\ z_{ss} \end{bmatrix} + \begin{bmatrix} 0 \\ -1 \end{bmatrix} \theta_{ref} \tag{19}$$

From the second row in Equation 19:

$$0 = Cx_{ss} - \theta_{ref} \tag{20}$$

$$y_{ss} = \theta_{ref} \tag{21}$$

$$\theta_{ss} = \theta_{ref} \tag{22}$$

Equation 22 shows that if there is closed loop stability, the controller overcomes steady state error. A property stemming from the development of the integral state, validating the reasoning in section III-A.

Following this confirmation, the gains for the K matrix were then determined.

The first step in designing a state feedback controller was to ensure that the system was controllable. The system was controllable if the reachability matrix, W, is of full rank.

$$W = \begin{bmatrix} A & AB & A^2B & A^3B \end{bmatrix} \tag{23}$$

$$\text{rank}(W) = 4 \tag{24}$$

The reachability matrix was of full rank, meaning that all the rows were linearly independent, therefore the system was controllable, implying it could be initialised at any state and be driven towards a reference value provided a suitable controller was designed.

To design a suitable controller, the system was put into canonical form, which can be thought of as a coordinate transform, to aid in the design of the K matrix seen in Equation 17. Canonical form has the general form:

$$A_t = \begin{bmatrix} -a_1 & -a_2 & -a_3 & \cdots & -a_n \\ 1 & 0 & 0 & \cdots & 0 \\ 0 & 1 & 0 & \cdots & 0 \\ \vdots & \vdots & \ddots & \ddots & \vdots \\ 0 & 0 & 0 & 1 & 0 \end{bmatrix}, \quad B_t = \begin{bmatrix} 1 \\ 0 \\ \vdots \\ 0 \end{bmatrix} \tag{25}$$

The coefficients of the characteristic polynomial of the A matrix were used to obtain the canonical form, A_t:

$$CP = det\,(sI - A) \tag{26}$$

$$CP = s^4 + 0.05897s^3 + 6.958 \times 10^{-5}s^2 \tag{27}$$

Using this result, the canonical form of A and B became:

$$A_t = \begin{bmatrix} -0.059 & 6.958 \times 10^{-5} & 0 & 0 \\ 1 & 0 & 0 & 0 \\ 0 & 1 & 0 & 0 \\ 0 & 0 & 1 & 0 \end{bmatrix} B_t = \begin{bmatrix} 1 \\ 0 \\ 0 \\ 0 \end{bmatrix} \tag{28}$$

The canonical form also had to be reachable:

$$W_t = \begin{bmatrix} A_t & A_tB_t & A_t^2B_t & A_t^3B_t \end{bmatrix} \tag{29}$$

$$\text{rank}(W_t) = 4 \tag{30}$$

The original state space form, Equation 15, and its canonical form, Equation 28, were both derived and were both shown to be reachable as their respective reachability matrices were of full rank.

As the system was fourth order, there were 4 poles that had to be placed. To design the controller so that the system had tunable characteristics, such as overshoot and settling time, the system was modelled as the product of a second order system and a first order system raised to the power of $G-2$ where G is the order of the system. The poles of the first order system were placed a distance, N, further to the left of the second order poles so that they had a negligible effect on the response characteristics of the system. This method allowed the system to be designed as if it were a second order system, where the poles have physical relationships, seen in Equation 31 :

$$\begin{aligned} &(s + N\zeta\omega_n)^2\ (s^2 + 2\omega_n\zeta s + \omega_n^2) \\ &\qquad = s^4 + p_1s^3 + p_2s^2 + p_3s + p_4 \end{aligned} \tag{31}$$

Let $a = N\zeta\omega_n$.

Expanding out Equation 31 resulted in the following expressions for the poles:

$$p_1 = 2a + 2\zeta\omega_n \tag{32}$$

$$p_2 = a^2 + 4a\zeta\omega_n + {\omega_n}^2 \tag{33}$$

$$p_3 = 2a^2\zeta\omega_n + 2a{\omega_n}^2 \tag{34}$$

$$p_4 = a^2{\omega_n}^2 \tag{35}$$

$$P = \begin{bmatrix} p_1 & p_2 & p_3 & p_4 \end{bmatrix}$$

The values for P were then obtained through the desired characteristics of the system.

As the controller was not adaptive, i.e. the K matrix didn't change depending on what the input reference pitch is, the characteristics of the system would be constant, and therefore it's imperative that the controller was designed with that in mind. This essentially translates to being forced to design the controller to the 'worst' case, i.e. the largest potential pitch reference value.

The maximum pitch angle of the Learjet 25 is not publicly available information. A standard subsonic business jet would very rarely exceed 20°, especially in cruise. Therefore, 20° was set as the maximum pitch reference value.

It is imperative for a pitch control autopilot to not overshoot, M_P, the reference pitch by too much, otherwise it could cause potential stalling of the aircraft. The settling time, T_s, of the Learjet when changing pitch cannot be too quick as it could cause excessive stress on the aircraft frame as well as passenger discomfort, this was helped by the fact that the controller would only be used in cruise flight where quick changes in pitch aren't required. The settling time was selected with a 20° reference pitch in mind. One second for every degree of pitch is reasonable and comfortable, therefore 20 seconds was selected for the settling time. An overshoot of 0.5% was selected to ensure minimal overshoot. The desired system response characteristics are outlined in Table III.

TABLE III: System Behaviour

Settling Time (T_S) [s]	Overshoot (M_P) [%]
20	0.5

From the desired M_P and T_s the damping ratio, ζ, and natural frequency, ω_n were then calculated using the following equations:

$$\zeta = \frac{-\ln(M_P)}{\sqrt{\pi^2 + \ln^2(M_P)}}$$

$$\zeta = 0.86\,[-] \tag{36}$$

$$\omega_n = \frac{3.92}{\zeta T_S} \tag{37}$$

$$\omega_n = 0.23\,\mathrm{rad/s} \tag{38}$$

The weaker first order poles were placed $N = 5$ times further left, the values obtained in Equation 36 and 38 were then substituted into Equations 32 - 35 to give the following values for the P matrix:

$$p_1 = 2.3520 \tag{39}$$

$$p_2 = 1.7819 \tag{40}$$

$$p_3 = 0.4807 \tag{41}$$

$$p_4 = 0.0511 \tag{42}$$

The canonical gain matrix was then formed using the following relationship:

$$K_t = \begin{bmatrix} p_1 & p_2 & p_3 & p_4 \end{bmatrix} + \begin{bmatrix} -a_1 & -a_2 & -a_3 & -a_4 \end{bmatrix} \tag{43}$$

$$K_t = \begin{bmatrix} 9.34902 & 28.91385 & 33.92901 & 19.27561 \end{bmatrix} \tag{44}$$

The transformation matrix from canonical form back to the original system was given by the relation:

$$T = W_t\, W^{-1} \tag{45}$$

The gain matrix for the controller in the original system was then given by the following:

$$K = K_t\, T \tag{46}$$

$$K = \begin{bmatrix} -0.0004 & -2.3128 & -0.0036 & 0.0004 \end{bmatrix} \times 10^5 \tag{47}$$

C. Stability

The stability of the closed loop dynamics were then tested to confirm that the controller, developed in section III-B, made the system stable. A state space system is deemed stable if, and only if, all the eigenvalues of A, the state matrix, have negative real parts. The addition of the controller changes the state matrix to $A - BK$. The eigenvalues were then calculated by finding solutions to Equation 48.

$$det\big((A - BK) - \lambda I\big) \tag{48}$$

$$\lambda_1 = -0.1960 + 0.1215i \tag{49}$$

$$\lambda_2 = -0.1960 - 0.1215i \tag{50}$$

$$\lambda_3 = -0.1470 + 0.0000i \tag{51}$$

$$\lambda_4 = -0.1470 + 0.0000i \tag{52}$$

All the eigenvalues or poles of the closed loop system had negative real parts, which confirmed that the system was stable.

D. Controller Validation

The controller was then validated through a range of testing. Ideally, the linear controller that was designed would be tested against the non-linear dynamics to see how applicable it would be in reality. Testing against the 6DOF equations, however, was not in scope due to the complexity and technical knowledge that would be required to do so. The coupled nature of the equations presents the largest challenge.

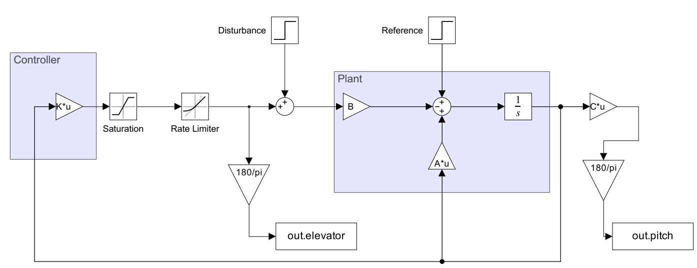

Fig. 2: SIMULINK Model

1) Reference Tracking

The initial validation was a simple reference tracking from an initial pitch of $\theta(0) = 0$.

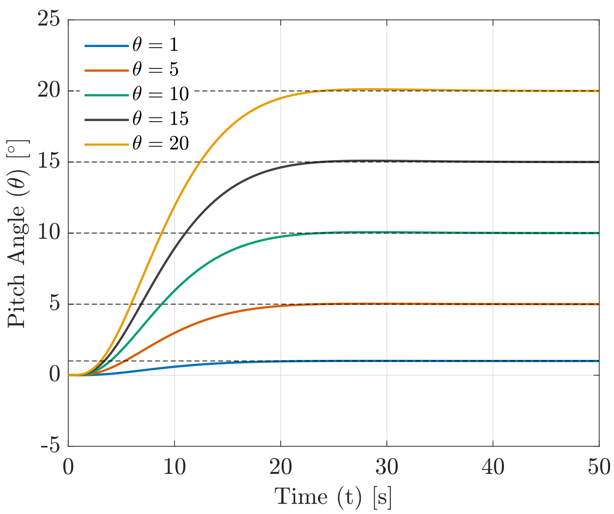

Fig. 3: Learjet 25 tracking various reference pitches from an initial $\theta(0) = 0°$. $N = 5$, $M_P = 0.5\%$, $T_S = 20$

The results from Figure 3 showed that the reference pitch was tracked well with no steady state error, with minimal overshoot, and the settling time behaved as designed.

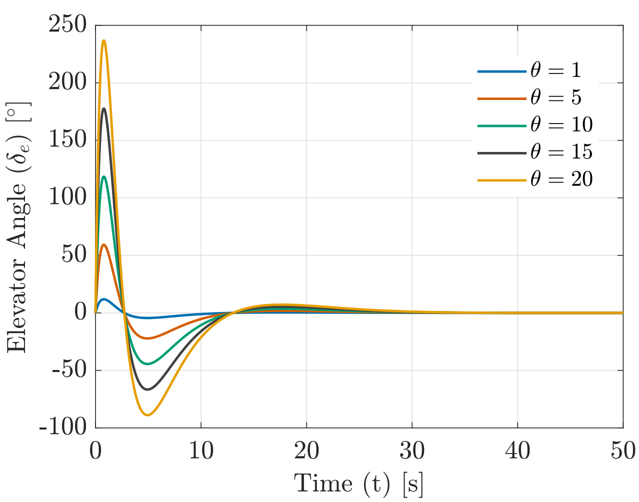

Fig. 4: Learjet 25 elevator deflection to obtain reference pitches. $\delta_e(0) = 0°$ $N = 5$, $M_P = 0.5\%$, $T_S = 20$

Figure 4 shows the elevator angle that was demanded from the controller to achieve the pitch results in Figure 3. It was obvious that this was completely unrealistic, as a typical elevator deflection is 30° nose up and 17° nose down [5]. The reasons for this elevator behaviour were not obvious. The model simplification was likely to be the reason, as there were a lot of simplifications and assumptions made to take the six degrees of freedom, highly non-linear, coupled equations down to longitudinal linearised versions. Ultimately, the more assumptions that are made; the less the equations reflect reality, which is likely what was happening in this instance.

After further testing, the elevator angle that was demanded from the controller was found to have a high dependence on N, the scaling distance used to place the weaker first order poles. Therefore, the location of the weaker first order poles was significant.

Through trial and error testing, it was found that by setting $N = 0.75$ and by keeping the overshoot and settling time the same, the elevator angle behaved in a much more realistic way:

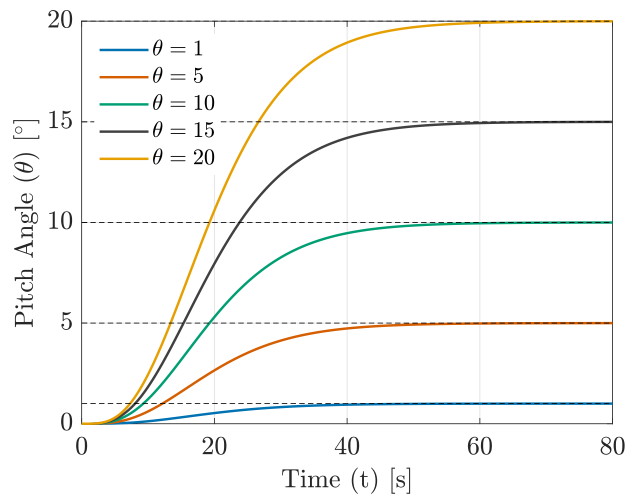

Fig. 5: Learjet 25 tracking various reference pitches from an initial $\theta(0) = 0°$. $N = 0.75$, $M_P = 0.5\%$, $T_S = 20$

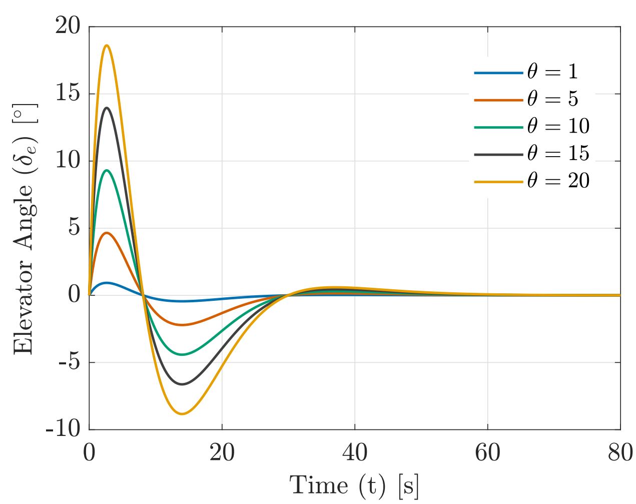

Fig. 6: Learjet 25 elevator deflection to obtain reference pitches. $\delta_e(0) = 0°$ $N = 0.75$, $M_P = 0.5\%$, $T_S = 20$

Figure 6 showed a much more realistic elevator deflection, which would be within the bounds of what is possible. However, it was found that the closer the first order poles were to the imaginary axis, i.e, the smaller the N value, the further the system strayed from the desired response characteristics outlined in Table III. This is illustrated in Figure 5, as the system had a much larger settling time, around 60 seconds.

Further research found that an optimisation method, linear quadratic regulation (LQR), could be implemented which offers an alternative to placing 'weaker' poles. It works by balancing performance to minimise a cost function. However, it is out of the scope of this report. Given that by setting $N = 0.75$, $M_P = 0.5\%$, $T_S = 20$, produces a controller that would *actually* work, despite it being far from optimal$_{\text{(probably)}}$, it is what was used for further validations.

2) Headwind

The next validation was to test the controller against an unknown constant disturbance. In the context of an aircraft pitch controller, this was modelled as a headwind of constant strength.

A constant headwind of unknown strength was modelled as to perturb the aircraft by $10°$, input as 0.175 rads. This would be an extreme headwind and the pilot would likely not fly in these conditions, but it illustrates well the power of the controller. In addition, if the controller was able to mitigate a headwind of this strength, it would be able to mitigate anything weaker. The disturbance was modelled as a step input at 40 seconds.

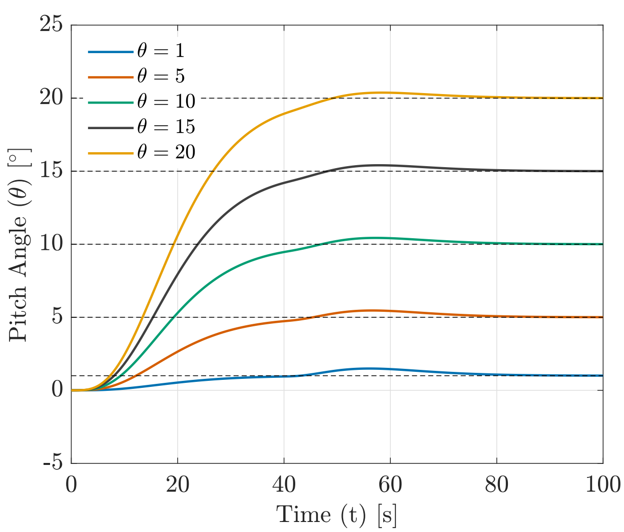

Fig. 7: Learjet 25 pitch response with a constant $10°$ pitch disturbance introduced at 40 seconds. $\theta(0) = 0°$. $N = 0.75$, $M_P = 0.5\%$, $T_S = 20$

The pitch response of the aircraft in Figure 7 shows excellent attenuation of the disturbance. The effects of the disturbance are clear to see in the extra overshoot of the response between 40-60 seconds when compared to Figure 3. Despite this constant disturbance, the controller was able to mitigate its effects completely as the steady state error goes to 0. This was confirmation that the controller design process and its implementation in section III-A was valid and correct.

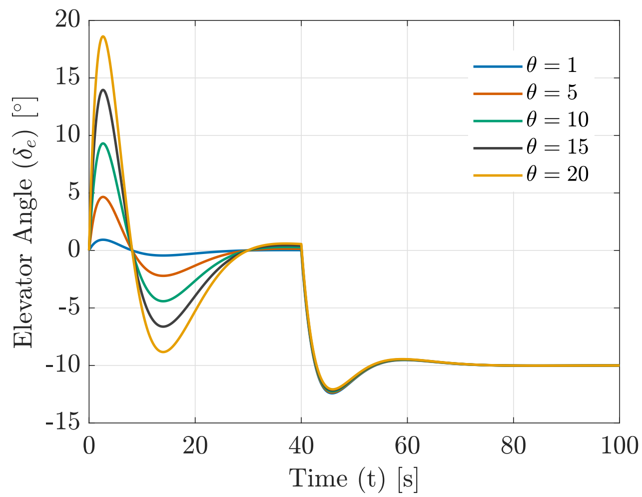

Fig. 8: Learjet 25 elevator response with a constant $10°$ pitch disturbance introduced at 40 seconds. $\delta_e(0) = 0°$ $N = 0.75$, $M_P = 0.5\%$, $T_S = 20$

The elevator response is shown in Figure 8. The elevator reacted immediately to the step input disturbance at 40 seconds, which was a reasonable assumption to make despite being an unrealistic behaviour due to the lag time between detection and response. The elevator was shown to deflect, overshoot slightly and reach a steady state value of $-10°$ despite the reference pitch. This result makes sense, by looking at the SIMULINK model in Figure 2, the controller and the disturbance were required to sum to 0 so that the steady state pitch, θ_{ss} equals the reference pitch,θ_{ref}. The result makes sense physically also, as the elevator acts to cancel out the pitching moment caused by the headwind by producing a pitching moment equal and opposite. The elevator overshoots to produce a pitching moment that corrects for the initial disturbance, and once corrected the elevator reaches a steady state value which simply cancels out the disturbance, hence the negative sign. However, the actual angle being equal and opposite is a property of the simplified model, as the area of the elevator and distance from the Learjet centre of mass have not been accounted for amongst many other things.

3) Turbulence

The next validation was to test against varying turbulence. Turbulence is caused by lots of factors. Essentially, they all disrupt the smooth flow of air around the wings, causing uneven pressure distributions and temporary changes in lift. The result being the 'bumpiness' that is associated with turbulence. It is the random nature and unpredictability of turbulence that makes it hard to model accurately, and so for this validation, a sinusoidal disturbance of $1°$ with an amplitude of 1 and frequency of $2\,\mathrm{rad/s}$ was used to simulate its effects. This was justified by assuming the strength of turbulence was much smaller than a headwind, and the 'bumpiness' translated to an oscillation. The reference pitch was selected to be $\theta_{ref} = 0$.

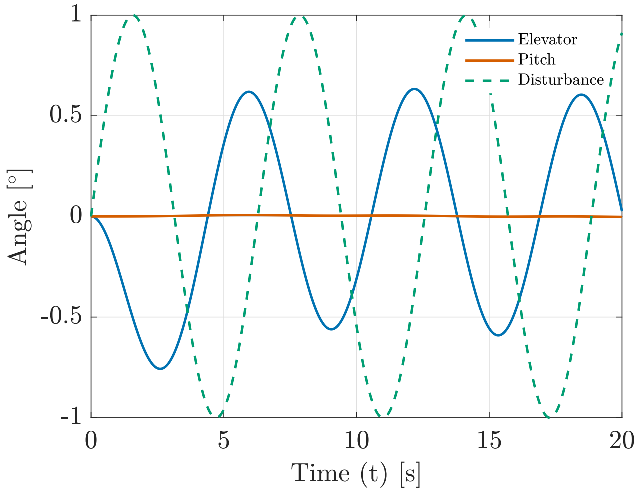

Fig. 9: Learjet 25 pitch and elevator response to sinusoidal turbulence. $\theta_{ref} = 0$. $N = 0.75$, $M_P = 0.5$ $T_S = 20$

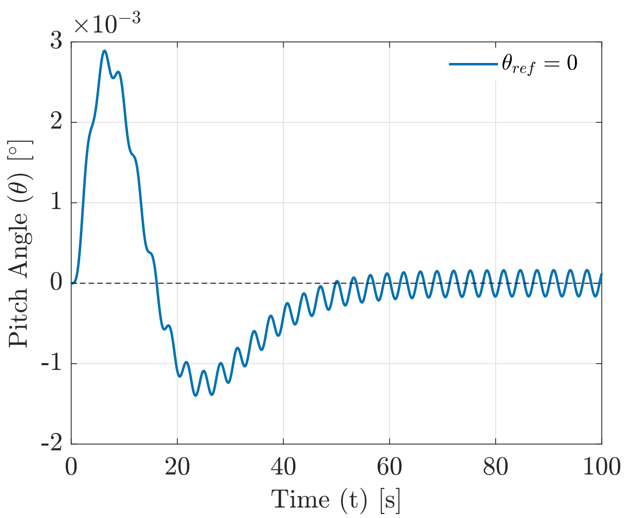

Fig. 10: Learjet 25 pitch response to sinusoidal turbulence. $\theta_{ref} = 0$. $N = 0.75$, $M_P = 0.5$ $T_S = 20$

Figure 9 shows the response of the Learjet. The results were impressive, the controller was able to mitigate the effects of the turbulence very well. The frequency of the turbulence means that the elevator did not need to reach an equal and opposite value to the disturbance itself, a result that was true in section III-D2. Figure 10 highlights the excellent attenuation of the turbulence, with the largest error in pitch measured $\approx 0.003°$. The phase difference between the elevator and the pitch of the Learjet was interesting, it was seen easily in Figure 9 and remained until the transient response decayed. In Figure 10, the steady state value was reached at around 80 seconds, the same as the result when testing against a constant disturbance seen in Figure 7. This result makes sense and highlights a shortcoming of the way that turbulence was simulated, as in an effort to simulate a varying disturbance, the constant frequency and amplitude meant that the turbulence was technically constant. This explains why Figure 10 has a very similar shape to Figure 8.

IV. Conclusion

This report designed and tested a pitch controller autopilot for a Learjet 25 to be used during the cruise stage of flight. Overall, the controller performed well and fulfilled the objective of controlling the pitch. The 6DOF aircraft equations of motion were simplified down to longitudinal linearised versions and put into state space form. An integral state was developed and successfully implemented and, once a state feedback controller was developed, achieved the goal of no steady state error. However, there were some key issues:

Ultimately, the model was a highly simplified version of the 6DOF equations. This resulted in the elevator deflection being completely unrealistic. By adjusting N the response behaved in a real way, although this meant that the settling time for the aircraft was approaching 60 seconds. Obviously this would not be ideal, and would likely not be good enough, but because it *actually* worked, i.e. the elevator wouldn't break, the configuration was deemed best.

The time taken between system response and controller input, i.e. how quickly the elevator was able to react, was assumed to be instant. This would not be the case and would be a very important parameter in reality. Further work would include detailed analysis using frequency response to determine the phase margin of the system. Essentially, how slow the controller is able to react to a disturbance before the system becomes unstable.

A limitation of state feedback, is that it requires perfect knowledge of all the states. This might not be possible in some situations. Another avenue for potential further work, would be motivation for the development of an observer, that uses state estimation to control.

References

[1] R. Nelson, *Flight Stability and Automatic Control*, ser. Aerospace Science & Technology. WCB/McGraw Hill, 1998. [Online]. Available: https://books.google.com.au/books?id=Uzs8PgAACAAJ

[2] T. Yechout and S. Morris, *Introduction to Aircraft Flight Mechanics*, ser. AIAA education series. American Institute of Aeronautics and Astronautics, 2003. [Online]. Available: https://books.google.com.au/books?id=TJlTAAAAMAAJ

[3] University of Michigan - Control Tutorials for MATLAB and Simulink. (2024) Aircraft pitch: System modeling. Accessed on April 29, 2024. [Online]. Available: https://ctms.engin.umich.edu/CTMS/index.php?example=AircraftPitch&section=SystemModeling

[4] D. Hull, *Fundamentals of Airplane Flight Mechanics*. Springer Berlin Heidelberg, 2010. [Online]. Available: https://books.google.com.au/books?id=vNyccQAACAAJ

[5] Airbus, *A320 Flight Controls*, 2024. [Online]. Available: https://www.smartcockpit.com/docs/A320-Flight_Controls.pdf